Food and Bioprocess Technology (2026) 19:352
https://doi.org/10.1007/s11947-026-04441-8

RESEARCH

# Process Intensification of Anthocyanin Recovery and Fouling Mitigation from Blueberry Pomace via Ultrasound-Integrated Membrane Processing

**Emel Yilmaz**[1] · **Irem Damar**[1] · **Orazgul Garagulyyeva**[1]

Received: 24 March 2026 / Accepted: 1 June 2026
© The Author(s) 2026

## Abstract

This study evaluated the performance of ultrasound-assisted membrane processes for the recovery of anthocyanins from blueberry pomace extract (BPE). Ultrasound was applied both as a pretreatment and as an integrated assistance during ultrafiltration (UF) to improve membrane performance and bioactive compound recovery. Prior to UF, microfiltration (MF) was applied to untreated BPE, during which permeate flux declined by 85%; ultrasound pretreatment reduced this decline to 79.4%, indicating mitigation of early-stage fouling. In UF systems, ultrasound pretreatment (US-pretreatment) increased the initial permeate flux by 8.83% in UF and by 35% in ultrasound-assisted UF (UA-UF). Total resistance was highest for UF of untreated BPE and lowest for UA-UF of US-pretreated BPE, while ultrasound integration reduced cake layer resistance by up to 37%. US-pretreatment significantly enhanced total phenolic, flavonoid, and monomeric anthocyanin contents of BPE ($p < 0.05$). Permeate fractions also exhibited improved bioactive compound transmission, with total phenolic content and DPPH antioxidant capacity in UA-UF permeates increasing by 12.7% and 8.96%, respectively, compared to UF. HPLC analysis confirmed that US-pretreatment increased total anthocyanin recovery without altering the relative anthocyanin profile. Antioxidant evaluation revealed assay-dependent responses, with ABTS showing more pronounced enhancement than DPPH, reflecting mechanistic differences in radical scavenging behavior. Overall, the synergistic application of US-pretreatment and membrane processing improved extraction efficiency, reduced fouling development, and enhanced permeate enrichment. These findings demonstrate the potential of ultrasound-assisted membrane technology as a sustainable strategy for valorizing berry processing by-products into anthocyanin-rich functional ingredients.

**Keywords** Blueberry pomace · Anthocyanins · Ultrasound · Ultrasound-assisted ultrafiltration · Membrane fouling

## Nomenclature

| | |
|---|---|
| $J_p$ | Permeate flux (kg $m^{-2}$ $h^{-1}$) |
| $L_p$ | Hydraulic permeability (kg $m^{-2}$ $h^{-1}$ $bar^{-1}$) |
| TMP | Transmembrane pressure (bar) |
| $R_t$ | Total resistance ($m^{-1}$) |
| $R_m$ | Membrane resistance ($m^{-1}$) |
| $R_c$ | Cake layer resistance ($m^{-1}$) |
| $R_{frev}$ | Reversible fouling resistance ($m^{-1}$) |
| $R_{firr}$ | Irreversible fouling resistance ($m^{-1}$) |
| UF | Ultrafiltration |
| UA-UF | Ultrasound-assisted ultrafiltration |
| MF | Microfiltration |
| BPE | Blueberry pomace extract |
| TPC | Total phenolic content |
| TFC | Total flavonoid content |
| TMAC | Total monomeric anthocyanin content |
| TAC | Total antioxidant capacity |
| PES | Polyethersulfone |

## Introduction

Blueberry (*Vaccinium myrtillus* L.) is a dark-colored fruit rich in phenolic compounds, particularly anthocyanins, which contribute to its antioxidant properties and potential applications as natural colorants and functional food ingredients (Duan et al., 2022; Tran & Tran, 2021). Blueberries also contain various bioactive constituents, including flavonoids, organic acids, and dietary fibers, supporting their relevance

✉ Emel Yilmaz
emelograsici@trakya.edu.tr

[1] Department of Food Engineering, Faculty of Engineering, Trakya University, 22180 Edirne, Turkey

Published online: 09 June 2026

as a valuable raw material for food processing applications (Bai et al., 2023).

Approximately 50% of blueberries are processed into juice or related products (Xie et al., 2022), generating pomace that is commonly treated as waste or used as animal feed, with associated economic and environmental burdens (Avram et al., 2017; Huang et al., 2025; Zhang et al., 2023). However, blueberry pomace retains substantial value as a source of bioactive compounds and dietary fibers (Irigoytia et al., 2022). It has been reported to contain 60.8% insoluble and 14.6% soluble dietary fiber, alongside sugars, protein, fat, and high anthocyanin levels (6444.5 µg/g), as well as polysaccharides such as pectin, xyloglucan, arabinoxylan, and mannan. Because anthocyanins are concentrated in the skins, a considerable fraction remains in the pomace after juice processing (Avram et al., 2017).

Membrane-based filtration is widely used to recover, fractionate, and purify bioactives from fruit and vegetable by-products as a non-thermal alternative that can preserve heat-sensitive compounds and enable compact, modular processing (Li & Chase, 2010). A key limitation is membrane fouling, which drives flux decline and increases operating costs (Lu et al., 2021). Membrane fouling can occur through several mechanisms, including pore blocking, adsorption, scaling, cake layer formation, and biological deposition. Accordingly, various mitigation strategies have been developed, such as feed pretreatment (e.g., coagulation, flocculation, and clarification), optimization of operating conditions (e.g., temperature, pH, and pressure), and chemical cleaning methods (Qasim et al., 2018).

Ultrasound integration into membrane systems ("acoustic filtration") has emerged as an approach to limit fouling and improve flux performance. The underpinning mechanism is acoustic cavitation, involving the formation and collapse of microbubbles that generate intense local conditions and physical effects (Chemat & Khan, 2011; Vinatoru et al., 2017). Ultrasound-assisted membrane processes enhance hydrodynamic conditions near the membrane surface by increasing turbulence and shear forces, promoting back-diffusion of accumulated particles, and thereby mitigating fouling through reduced concentration polarization and improved mass transport (Córdova et al., 2020; Naji et al., 2021).

Previous studies have demonstrated that ultrasound can be effectively applied both as a pretreatment to feed solutions and as an in-line assistance during membrane filtration. Ultrasonic pretreatment increased the recovery of total phenolic compounds and anthocyanins and improved the initial permeate flux during the microfiltration of Sohiong fruit juice (Pradhan et al., 2022). Applying ultrasound during filtration has also improved performance in other matrices: enhanced permeate flux in carrot juice clarification when ultrasound was applied to both feed and module (Hemmati et al., 2021), reduced cake layer thickness during pomegranate juice clarification (Aghdam et al., 2015), and improved flux with reduced cake formation and total resistance during ultrasound-assisted ultrafiltration of green tea extract (dos Santos Sousa et al., 2016). Ultrasound has additionally been reported as effective for cleaning ceramic and polyethersulfone (PES) membranes, with low-frequency operation improving flux recovery (Lamminen et al., 2004; Luján-Facundo et al., 2017; Maskooki et al., 2008; Wang et al., 2013). Collectively, these findings indicate that ultrasound-assisted membrane processing is a promising route for flux enhancement and fouling control.

Therefore, the main objective of this study is to evaluate the effect of ultrasound applied both as a pretreatment and integrated into a PES ultrafiltration system on membrane process performance and anthocyanin recovery from blueberry pomace extract. The study investigates permeate flux behavior, fouling characteristics based on resistance-in-series analysis, and changes in total phenolic, flavonoid, and anthocyanin contents. In addition, individual anthocyanin profiles are analyzed to determine the impact of ultrasound-assisted membrane processing on compositional distribution. By combining process intensification with detailed compositional analysis, this work aims to propose an effective and sustainable valorization strategy for the recovery of high-value anthocyanins from blueberry pomace.

## Material and Methods

### Materials

#### Chemicals and Reagents

Folin-Ciocalteu reagent, anhydrous sodium carbonate, sodium nitrite, aluminum chloride hexahydrate and sodium hydroxide, potassium chloride and sodium acetate hydroxide, 2,2′-azinobis-(3-ethylbenzothiazoline-6-sulfonic acid) (ABTS), 2,2-diphenyl-1-picrylhydrazyl (DPPH), potassium persulfate, 6-hydroxy-2,5,7,8-tetramethylchroman-2-carboxylic acid (Trolox), ethanol, methanol, gallic acid, and (+)-catechin were purchased from Sigma (St. Louis, MO, USA). All solvents used for analytical determinations were of HPLC grade. Ultrapure water (conductivity < 0.5 $\mu S\,cm^{-1}$), produced using a PURELAB Option-Q (ELGA LabWater, UK), was used in all membrane experiments.

#### Feed Solution Preparation

Blueberry fruits were obtained from a local producer in Edirne, Turkey. The samples were processed using a mechanical juicer (Schwartz, SWJ 7770, Turkey), yielding blueberry juice with an efficiency of 82.54% (w/w) based

on the initial fresh weight. As a result of the juicing process, pomace was generated at approximately 7–8% (w/w). The obtained pomace was pre-frozen at – 18 °C for 24 h and subsequently freeze-dried using a lyophilizer (Labconco, FreeZone 6 Plus, Kansas City, KS, USA). Following lyophilization, dry pomace was obtained and ground into powder. The powdered pomace was then dissolved in distilled water at a solid-to-liquid ratio of 1:100 (w/v) and incubated in a shaking water bath (Memmert, Schwabach, Germany) at 50 °C for 2 h. The resulting extract was filtered, and blueberry pomace extract (BPE) was obtained at a concentration of 10 g/L.

## Methods

To investigate the effect of ultrasound on the UF process, two distinct strategies were employed: ultrasound was applied either as a pretreatment to the BPE feed or integrated into the UF module. A schematic representation of the UF experiments is shown in Fig. 1.

### Ultrasound Pretreatment

Ultrasound pretreatment was applied to the BPE sample using a probe-type ultrasonic homogenizer (Bandelin, Sonopuls HD 4200, Germany) equipped with a 9-mm diameter probe (TS 109). The system operated at a frequency of 20 kHz and a nominal maximum power of 200 W. Ultrasound was applied at an amplitude of 50% (≈ 100 µm) for 5 min. The ultrasonic probe was immersed to a depth of approximately 5 cm into the sample contained in a double-walled extraction tube (total liquid height: 10 cm). The process was conducted at a constant temperature (25 ± 1 °C), maintained using an ice–water mixture in the double-walled extraction tube.

### Microfiltration (MF)

In the MF of BPE samples, a CF042 stainless steel 316 L cross-flow module (Sterlitech Corporation, Kent, WA, USA) was used. BPE samples with and without ultrasound pretreatment were passed through a MF membrane

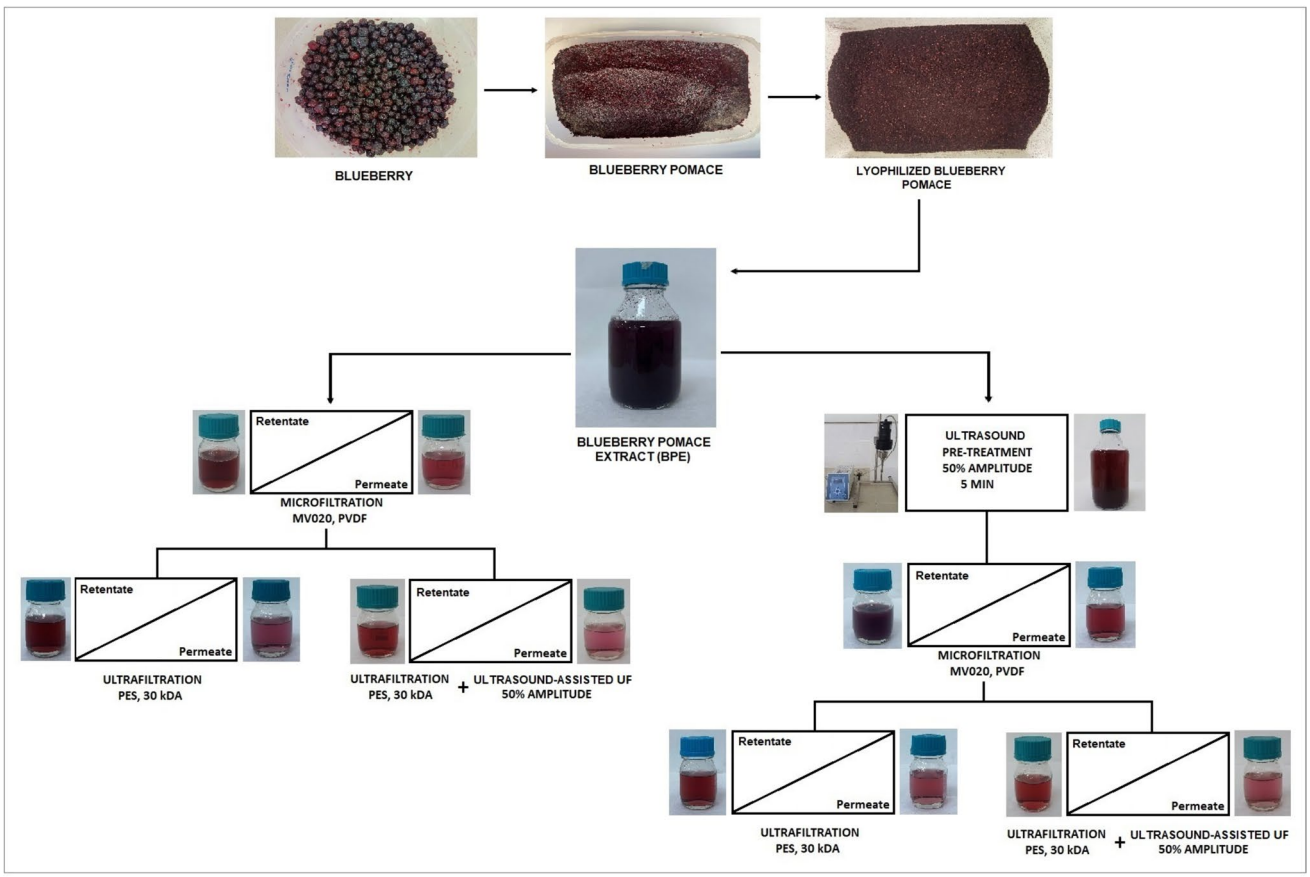



**Fig. 1** Experimental setup of ultrafiltration (UF) experiments used to evaluate the effects of ultrasound pretreatment and in-line ultrasound integration on membrane fouling during anthocyanin recovery from blueberry pomace extract

(Microdyn Nadir, PM, MV020, PVDF) with a pore size of 0.2 µm prior to the UF process to remove suspended solids. MF was performed at a feed flow rate of 40 L $h^{-1}$, at 25 °C, and under 1.5 bar pressure. The permeate obtained from the MF membrane was used as the feed for the UF system.

### Ultrafiltration and Ultrasound-Assisted Ultrafiltration Process

UF was performed either without ultrasound (UF) or with in situ ultrasound applied at 50% amplitude (UA-UF) to assess the effects of US-pretreatment and ultrasound integration on membrane fouling and filtration performance.

UF and UA-UF of BPE were conducted in the same cross-flow filtration module used for MF. Flat-sheet PES membranes (MK, Synder Filtration, USA) with a 30-kDa MWCO were used. For UA-UF, ultrasound was applied using a probe-type ultrasonic homogenizer (Bandelin, Sonopuls HD 4200, Germany) operating at a frequency of 20 kHz and a nominal maximum power of 200 W. The system was operated at 50% amplitude using a 9-mm probe (TS 109). The ultrasonic probe was immersed to a depth of approximately 6 cm from the liquid surface, corresponding to a distance of approximately 6 cm from the bottom of the container (total liquid height: 12 cm). A schematic of the UA-UF system is shown in Fig. 2.

Prior to filtration, membranes were compacted by filtering distilled water at 40 L $h^{-1}$ for 30 min at 2 bar TMP. BPE was then filtered in batch concentration mode at 2 bar TMP and 25 ± 2 °C, using a peristaltic pump (Bimetron, Izmir, Turkey) at a feed flow rate of 40 L $h^{-1}$. Permeate was collected in a container placed on an analytical balance (Isolab, Istanbul, Turkey). The initial permeate flux ($J_p$) was calculated from the permeate mass collected over time (Eq. 1):

$$J_p = \frac{W_p}{At} \quad (1)$$

where $J_p$ represents the permeate flux (kg $m^{-2}{\cdot}h^{-1}$), $W_p$ is the weight of the permeate (kg), $t$ is the time (h), and $A$ is the membrane surface area ($m^2$).

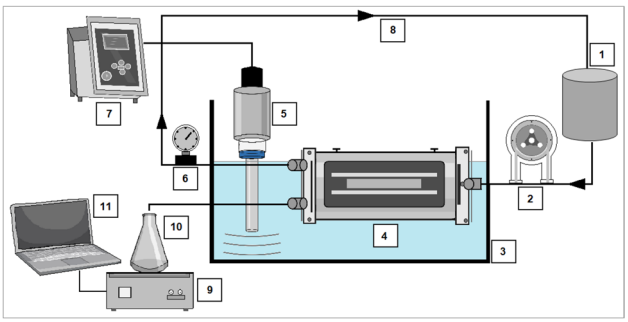



**Fig. 2** Schematic diagram of the ultrasound-assisted ultrafiltration system (1: feed tank, 2: peristaltic pump, 3: water-filled container, 4: membrane module, 5: ultrasonic probe, 6: pressure gauge, 7: generator, 8: retentate, 9: analytical balance, 10: permeate container, 11: computer)

**Hydraulic Permeability and Fouling Analysis** To determine the effect of ultrasound on fouling mechanisms during the UF process, the hydraulic permeability values of UF membranes with a 30-kDa MWCO were measured under constant operating conditions. For this purpose, hydraulic permeability of the membrane (kg $m^{-2}$ $h^{-1}$ $bar^{-1}$) was determined at 25 ± 2 °C and 40 L $h^{-1}$ flow rate by plotting the distilled water flow values against the applied TMP (1–1.5–2 bar) and was determined by the slope of the straight lines drawn on the resulting graph. The initial hydraulic permeability of the unused membrane was defined as $L_{p0}$. After the application of the BPE, the hydraulic permeability was recorded as $L_{p1}$. Following membrane rinsing with water, the permeability was defined as $L_{p2}$, and after chemical cleaning with 0.5% NaOH, the final permeability was recorded as $L_{p3}$. The water and chemical cleaning procedures were each performed for 30 min.

**Resistance-in-Series Analysis** Fouling resistances were determined based on the resistance-in-series model derived from Darcy's law, using the calculated hydraulic permeability values as described by Cassano et al. (2007) (Eq. 2).

$$J_p = \frac{\Delta P}{\mu R_t} \quad (2)$$

In this model, $J$ represents the water flux, $\Delta P$ denotes the transmembrane pressure (TMP), $\mu$ is the dynamic viscosity of the permeate, and $R_t$ refers to the total filtration resistance. The total resistance $R_t$ consists of several components: the intrinsic membrane resistance ($R_m$), cake layer resistance ($R_c$), reversible fouling resistance ($R_{frev}$), and irreversible fouling resistance ($R_{firr}$).

### Chemical Characterization

**Determination of Total Phenolic Content (TPC)** The TPC of the samples was determined using a previously reported method (Prevete et al., 2024), with slight modifications. For the analysis, 1 mL of appropriately diluted sample, 5 mL of 0.1 N Folin-Ciocalteu reagent, and 4 mL of saturated sodium carbonate solution (75 mg/L) were added to a test tube and mixed using a vortex. The mixture was then incubated in

a water bath at 50 °C for 5 min and allowed to cool. The absorbance of the cooled tubes was measured at 760 nm using a spectrophotometer (Shimadzu, Kyoto, Japan). The results were calculated using a standard gallic acid calibration curve ($y = 0.011x$, $R^2 = 0.9948$) and expressed as g gallic acid equivalents per kg of lyophilized weight (LW).

**Determination of Total Flavonoid Content (TFC)** The TFC of the samples was determined using the method proposed by Dewanto et al. (2002). A volume of 250 µL of appropriately diluted sample was mixed with 75 µL of 5% $NaNO_2$ solution. After 6 min, 150 µL of 10% $AlCl_3$ solution was added, followed by 500 µL of 1 M NaOH solution after an additional 5 min. The mixture was then brought to a final volume of 2.5 mL with distilled water. The absorbance was measured at 510 nm using a spectrophotometer (Shimadzu, Kyoto, Japan). The results were calculated using a standard catechin calibration curve ($y = 0.0014x$, $R^2 = 0.9919$) and expressed as g catechin equivalents per kg of LW.

**Determination of Total Monomeric Anthocyanin Content (TMAC)** For the determination of TMAC, the samples were appropriately diluted with buffer solutions at pH 1.0 and pH 4.5. The diluted samples were left to stand at room temperature for 15 min and then filtered through 0.45-µm PVDF syringe filters. The absorbance values of the samples were measured at 514 nm and 700 nm using a spectrophotometer (Giusti & Wrolstad, 2001). The total monomeric anthocyanin content was calculated using Eq. 3 and expressed as g malvidin-3-glucoside (Mv-3-glu) per kg of LW.

$$\mathrm{TMAC} = \frac{\left(\left(A_{514} - A_{700}\right)_{\mathrm{pH1.0}} - \left(A_{514} - A_{700}\right)_{\mathrm{pH4.5}}\right) \times \mathrm{MW} \times \mathrm{DF} \times 10^3}{\varepsilon \times l} \quad (3)$$

where $A$ = absorbance; MW = molecular weight of Mv-3-glu (493.2 g $mol^{-1}$); DF = dilution factor; $l$ = path length of spectrophotometer cuvette (cm); $\varepsilon$ = 28 000 molar extinction coefficients for Mv-3-glu (L $mol^{-1}$ $cm^{-1}$); and $10^3$ = factor for conversion from g to mg.

**Identification and Quantification of Individual Anthocyanins by HPLC** Anthocyanin composition was analyzed by high-performance liquid chromatography (HPLC) using a modified method based on Nour et al. (2013). The analyses were performed with an Agilent 1200 HPLC system (Agilent Technologies, Santa Clara, CA, USA) equipped with a C18 reversed-phase column (150 × 4.6 mm, 3 µm). The separation was carried out at 40 °C with detection at 530 nm. The mobile phase consisted of solvent A: 10% acetonitrile in water containing 1% formic acid, and solvent B: 89% acetonitrile in water containing 1% formic acid. The flow rate was set at 0.5 ml/min. A gradient elution program was applied as follows: 0 min (97% A), 5–15 min (95% A), 20 min (90% A), 25 min (80% A), 28 min (75% A), 30 min (50% A), 35–40 min (97% A). Anthocyanins were identified by comparing retention times and spectra with standards, including malvidin-3-O-galactoside chloride, malvidin-3-O-glucoside chloride, delphinidin-3-O-galactoside chloride, delphinidin-3-glucoside, delphinidin-3-rutinoside, cyanidin-3-glucoside, cyanidin-3-rutioside, and peonidin-3-glucoside. Quantification was performed using calibration curves generated for each standard compound and results expressed as mg/kg.

**Determination of Total Antioxidant Capacity (TAC)** The TAC of the samples was determined using two complementary methods based on $DPPH^{\bullet}$ and $ABTS^{*+}$ radicals. In the DPPH assay, a stock solution was prepared by dissolving 24 mg of DPPH in 100 mL of methanol. Prior to the analysis, the stock solution was diluted with methanol to adjust its absorbance to approximately 0.800 at 517 nm. For the assay, 150 µL of the sample was mixed with 2850 µL of the $DPPH^{\bullet}$ solution, and the decrease in absorbance was measured at 517 nm after the reaction (Thaipong et al., 2006). In the ABTS assay, the ABTS radical cation ($ABTS^{*+}$) was generated by mixing 7 mM ABTS with 2.45 mM $K_2S_2O_8$, followed by incubation in the dark at room temperature for 16 h. The resulting solution was then diluted with ethanol to an absorbance of 0.700 ± 0.02 at 734 nm. A volume of 30 µL of the sample was added to 3 mL of the $ABTS^{*+}$ solution, and the reduction in absorbance was recorded after 6 min (Re et al., 1999). The TAC was expressed as mmol Trolox equivalents (TE) per kg of LW based on standard Trolox calibration curves (for DPPH $y = 0.912x$, $R^2 = 0.9956$, for ABTS $y = 0.2728x$, $R^2 = 0.9958$).

### Statistical Analysis

Statistical analysis of the data was conducted using one-way analysis of variance (ANOVA) with IBM SPSS Statistics version 26 (SPSS, Inc., Chicago, IL). Differences between groups were determined using Duncan's multiple range test, while comparisons related to the ultrasound pretreatment applied to the extract samples were evaluated using the independent samples $t$-test, both at a 95% confidence level. All experiments were performed in triplicate, and the results are expressed as mean ± standard deviation ($n = 3$).

## Results and Discussion

### Effect of Ultrasound Pretreatment on Microfiltration Performance

The permeate flux profiles for untreated and US-pretreated BPE (Fig. 3) exhibited a typical microfiltration behavior characterized by a rapid initial decline followed by a more gradual decrease over time. For untreated BPE, the permeate flux decreased substantially during the filtration process (from approximately 254.14 to 38.23 kg $m^{-2}$ $h^{-1}$), with the most pronounced decline occurring within the first 10 min, indicating severe pore blocking at the early stage. In contrast, the US-pretreated sample showed a lower initial flux (154.86 kg $m^{-2}$ $h^{-1}$) but a noticeably slower rate of decline, reaching 32.29 kg $m^{-2}$ $h^{-1}$ at the end of filtration.

The temporal permeate flux profiles obtained for both samples followed a typical two-stage MF behavior, characterized by an initial rapid flux decline followed by a slower and more gradual decrease. The absence of a clear steady-state flux region is consistent with previous observations reported for the MF and UF of complex plant extracts (Ahmad et al., 2012). The initial sharp flux decline is generally attributed to pore blocking, while the subsequent gradual decrease is associated with cake layer formation on the membrane surface (Ehsani et al., 2021).

A comparative analysis of the permeate flux profiles clearly demonstrated that ultrasound pretreatment mitigated the severity of both the initial pore blocking and the subsequent fouling development during MF. The slower flux decline observed for the US-pretreated BPE indicates that ultrasound-induced structural modification of suspended particles and macromolecular components promoted the formation of a more porous and less compact fouling layer on the membrane surface, thereby facilitating permeate transport throughout the filtration process. US-pretreatment has been reported to improve permeate flux behavior during the MF of fruit juices by promoting the disruption of large particles in the feed solution and reducing the compressibility of the formed cake layer (Hemmati et al., 2021; Pradhan et al., 2022), which was consistent with the flux stabilization observed in the present study.

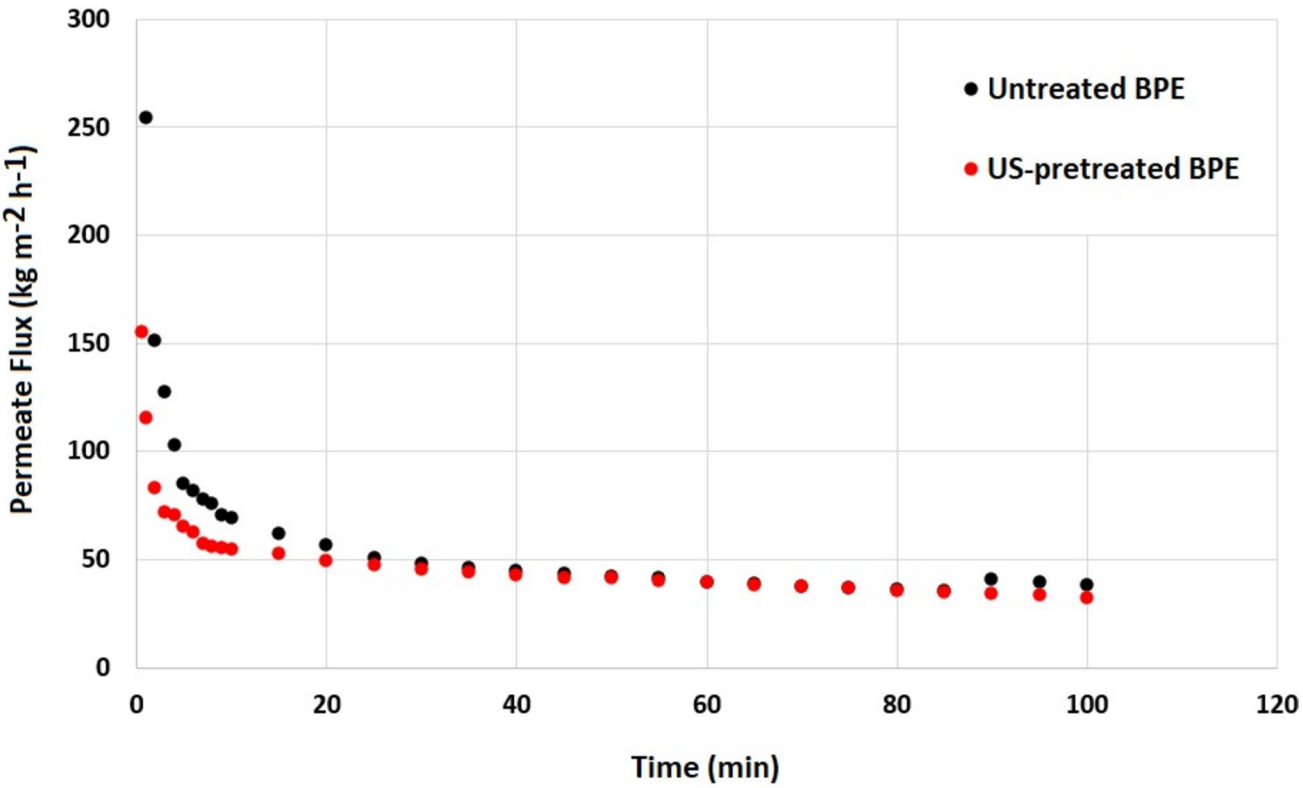



**Fig. 3** Permeate flux profiles during microfiltration of untreated and ultrasound-pretreated blueberry pomace extract

## Ultrafiltration and Ultrasound-Assisted Ultrafiltration Performance

### Permeate Flux Behavior

MF permeate samples were used as the feed for the UF step using a 30-kDa MWCO PES membrane (Fig. 4). For untreated BPE, the permeate flux decreased from 80.29 to 41.40 kg $m^{-2}$ $h^{-1}$ over 65 min. In contrast, UA-UF exhibited a higher initial flux (93.71 kg $m^{-2}$ $h^{-1}$) and a comparable final flux (46.71 kg $m^{-2}$ $h^{-1}$). Although UA-UF showed a sharper initial decline within the first 10 min, the subsequent flux decrease was markedly limited compared to UF. Overall, ultrasound integration improved the initial flux and contributed to a more stable flux profile during the later stages of filtration.

The faster initial decline in UA-UF (first 10 min) but slower decline thereafter indicates that ultrasound integration mainly affected later-stage fouling behavior, markedly slowing flux loss from the 10th min onward. This is consistent with cavitation-assisted foulant removal from the membrane surface (Ehsani et al., 2021), reduced concentration polarization (Naji et al., 2021), and enhanced turbulence/high shear promoting back-diffusion of accumulated particles to the feed (Córdova et al., 2020). The larger decline observed in UF after the 10th min (31.80%) suggests continued pore blockage and cake layer formation in the absence of ultrasound. Similar permeate flux benefits of ultrasound used as both pretreatment and filtration aid have been reported for carrot juice clarification (Hemmati et al., 2021). Lamminen et al. (2004) also showed that high power density and low frequency improve particle removal from membrane surfaces and increase permeate flux, while ceramic membranes can be ultrasonically cleaned over 70–620 kHz without structural damage.

For US-pretreated BPE, the permeate flux during UF decreased from 116.29 to 72.14 kg $m^{-2}$ $h^{-1}$ over 40 min. In UA-UF, a higher initial flux was observed (126.57 kg $m^{-2}$ $h^{-1}$), with a similar final flux (~73.43 kg $m^{-2}$ $h^{-1}$). Although UA-UF exhibited a more pronounced decline during the first 10 min, the subsequent flux decrease was lower compared to UF. Overall, ultrasound integration improved the initial flux but led to a more stabilized flux profile after the initial filtration stage.

Overall, ultrasound-assisted membrane processes mitigate fouling through removal of accumulated foulants, reduction of concentration polarization, and improved feed transport across the membrane (Naji et al., 2021). Although the

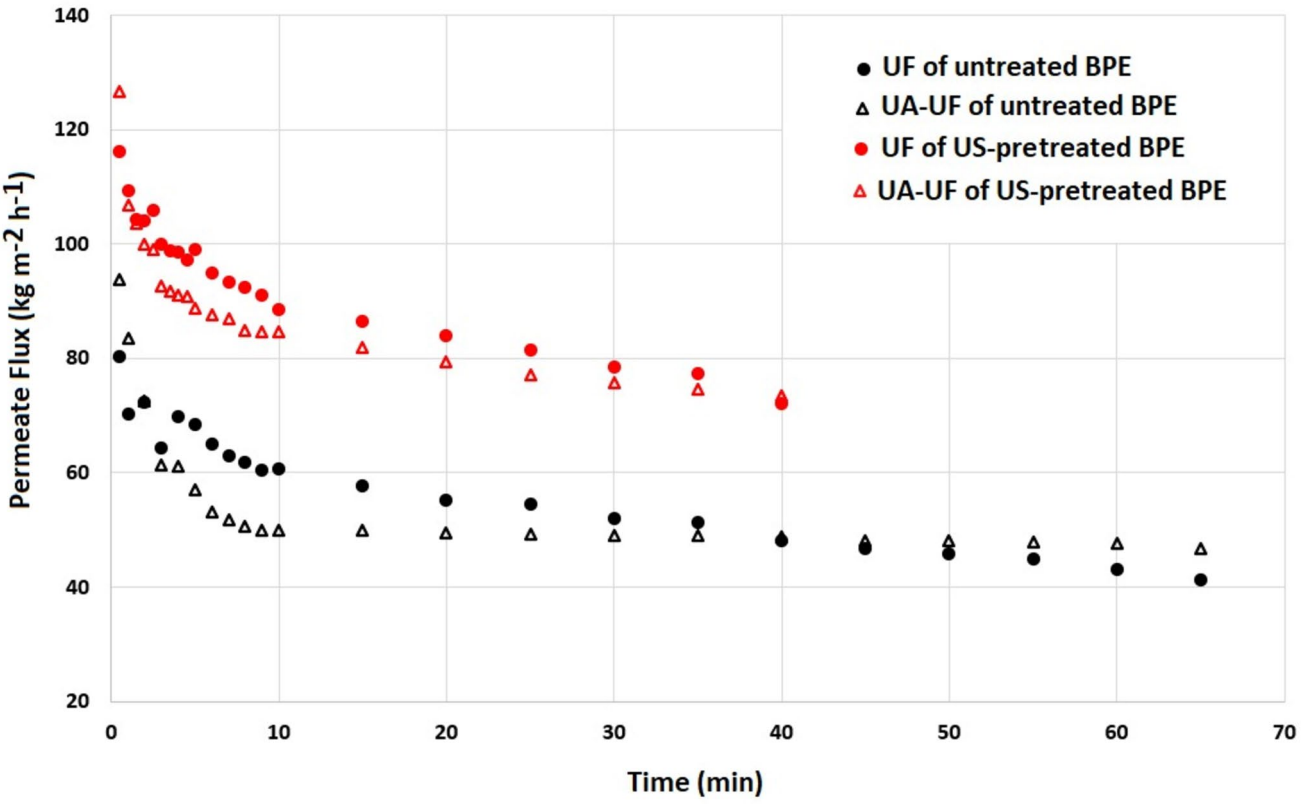



**Fig. 4** Comparative permeate flux profiles during ultrafiltration and ultrasound-assisted ultrafiltration of untreated and ultrasound-pretreated blueberry pomace extract

permeate flux in UA-UF decreased more sharply during the first 10 min, the subsequent flux decline was slower than in UF, indicating a more stable permeate flux profile after ultrasound integration. US-pretreatment also improved initial filtration conditions, likely by reducing extract viscosity and modifying foulant-forming components; this interpretation agrees with the reported relationship between higher feed viscosity, earlier concentration polarization, and earlier flux decline (Bacchin et al., 2006).

Based on the flux profiles, US-pretreatment improved the initial flux in both UF and UA-UF, and the effect was particularly pronounced in UA-UF, in which pretreatment yielded a 35% higher initial flux compared with untreated BPE. In addition, pretreatment was associated with lower total flux decline and lower first-10-min flux decline in both processes (relative to untreated BPE). While ultrasound had a more pronounced fouling-mitigation effect in non-pretreated samples, its effect after pretreatment was more balanced, and the combined use of pretreatment and ultrasound integration provided the most favorable overall filtration performance among the tested conditions.

### Hydraulic Permeability Behavior

Hydraulic permeability values were calculated to evaluate the effects of US-pretreatment and ultrasound integration into the UF system on membrane fouling behavior. The hydraulic permeability data were presented in Table 1. The $L_{p0}$ values of the clean membranes used in the UF experiments ranged from 63.33 to 65.60 kg $m^{-2}$ $h^{-1}$ $bar^{-1}$.

For untreated BPE, hydraulic permeability decreased by 53.44% after UF and by 48.8% after UA-UF. After water rinsing, hydraulic permeability recovery was 58.10% for UF and 59.01% for UA-UF. Following chemical cleaning with 0.5% NaOH, hydraulic permeability recovery increased to 77.30% and 92.48% for UF and UA-UF, respectively. For US-pretreated BPE, hydraulic permeability decreased by 48.37% after UF and by 42.30% after UA-UF. After water rinsing, hydraulic permeability recovery was 67.43% for UF and 69.80% for UA-UF. After chemical cleaning, the recovery values were 82.58% for UF and 87.64% for UA-UF.

Overall, comparison of UF and UA-UF indicates that ultrasound integration reduced hydraulic permeability loss for both untreated and US-pretreated BPE. The highest recovery after water rinsing was observed for UA-UF of US-pretreated BPE (69.80%), whereas the lowest recovery after chemical cleaning was obtained for UF of untreated BPE (77.30%), suggesting a stronger contribution of irreversible fouling under this condition. The highest post-chemical-cleaning recovery was obtained for UA-UF of untreated BPE (92.48%). These results indicate that ultrasound integration helped preserve hydraulic permeability and improved water permeability recovery after cleaning.

**Table 1** Hydraulic permeability of PES membrane during ultrafiltration and ultrasound-assisted ultrafiltration with and without ultrasound pretreatment

| Pretreatment | Filtration mode | Hydraulic permeability (kg $m^{-2}$ $h^{-1}$ $bar^{-1}$) | | | |
|---|---|---|---|---|---|
| | | $L_{p0}$ | $L_{p1}$ | $L_{p2}$ | $L_{p3}$ |
| Untreated | UF | 65.60 | 30.54 | 38.12 | 50.71 |
| | UA-UF | 63.33 | 32.43 | 37.37 | 58.57 |
| US-P | UF | 64.42 | 33.26 | 43.44 | 53.20 |
| | UA-UF | 64.74 | 37.35 | 45.19 | 56.74 |

*US-P* US-pretreatment, *UF* ultrafiltration, *UA-UF* ultrasound-assisted ultrafiltration, $L_{p0}$ initial hydraulic permeability of the unused membrane, $L_{p1}$ hydraulic permeability after BPE application, $L_{p2}$ hydraulic permeability after water rinsing, $L_{p3}$ hydraulic permeability after chemical cleaning with 0.5% NaOH

### Fouling Mechanisms Based on Resistance-in-Series Analysis

Permeate flux decline was analyzed using the resistance-in-series model. In this model, total resistance ($R_t$) was expressed as the sum of intrinsic membrane resistance ($R_m$), cake layer resistance ($R_c$), and reversible ($R_{frev}$) and irreversible ($R_{firr}$) fouling resistances; the sum of reversible and irreversible fouling resistances was defined as $R_f$ (Cassano et al., 2007). Membrane resistance values and their contributions to total resistance were presented in Table 2.

For untreated BPE, $R_t$ was $11.79 \times 10^{12}$ $m^{-1}$ in UF and decreased by 5.85% in UA-UF. Ultrasound integration reduced the contribution of cake layer resistance to total resistance, which contributed to the decrease in $R_t$. At the same time, the relative contribution of reversible fouling increased, whereas irreversible fouling decreased in UA-UF. For US-pretreated BPE, $R_t$ was $10.82 \times 10^{12}$ $m^{-1}$ in UF and decreased by 10.91% in UA-UF. Similar to untreated BPE, ultrasound integration reduced the contribution of $R_c/R_t$, while increasing the relative contribution of reversible fouling and lowering irreversible fouling.

The highest total resistance was observed in UF of untreated BPE. Ultrasound integration reduced cake layer formation during UF by 37% and 34% for untreated and US-pretreated BPE, respectively. The contribution of irreversible fouling resistance to total resistance was 13.66% in UF of untreated BPE and 10.90% in UF of US-pretreated BPE, while the corresponding values in UA-UF were 4.14% and 8.09%, respectively. These results indicate that ultrasound use during UF reduced both total resistance and the contribution of irreversible fouling under both pretreatment conditions, while shifting fouling behavior toward a more reversible character.

This behavior may be associated with ultrasound-induced particle size reduction/homogenization and

**Table 2** Resistance-in-series analysis of PES membrane under ultrafiltration and ultrasound-assisted ultrafiltration

| Pretreatment | Filtration mode | Resistance components ($\times 10^{12}$ $m^{-1}$) | | | | | Relative contribution (%) | | |
|---|---|---|---|---|---|---|---|---|---|
| | | $R_t$ | $R_m$ | $R_c$ | $R_{frev}$ | $R_{firr}$ | $R_m/R_t$ | $R_c/R_t$ | $R_f/R_t$ |
| Untreated | UF | 11.79 | 5.49 | 2.34 | 2.35 | 1.61 | 46.56 | 19.87 | 33.57 |
| | UA-UF | 11.10 | 5.68 | 1.47 | 3.49 | 0.46 | 51.20 | 13.23 | 35.56 |
| US-P | UF | 10.82 | 5.59 | 2.54 | 1.52 | 1.18 | 51.63 | 23.43 | 24.94 |
| | UA-UF | 9.64 | 5.56 | 1.67 | 1.62 | 0.78 | 57.70 | 17.34 | 24.96 |

*US-P* US-pretreatment, *UF* ultrafiltration, *UA-UF* ultrasound-assisted ultrafiltration, $R_t$ total resistance, $R_m$ the intrinsic membrane resistance, $R_c$ cake layer resistance, $R_{frev}$ reversible fouling resistance, $R_{firr}$ irreversible fouling resistance

disruption of the cake layer at the membrane surface. Ultrasound has been reported to increase permeate flux by breaking the cake layer on the membrane surface (Ahmad et al., 2012). Consistent with the hydraulic permeability results, the present findings suggest that ultrasound altered fouling behavior in a way that facilitated membrane cleaning and supported longer and more efficient filtration operation.

Similar findings have been reported in the literature. In pomegranate juice clarification, cake layer formation was identified as the dominant fouling mechanism in both ultrasound-assisted and conventional membrane processes, but cake formation was lower in the ultrasound-assisted system (Aghdam et al., 2015). Likewise, in the purification of polyphenols from green tea leaves, ultrasound-assisted ultrafiltration reduced total resistance by 44%, mainly by suppressing cake layer formation (dos Santos Sousa et al., 2016). In carrot juice membrane clarification, the highest total resistance was observed in the non-ultrasound system, while the lowest was obtained in ultrasound-assisted membrane filtration combined with ultrasound pretreatment; SEM images also showed more severe fouling in membranes operated without ultrasound and a thinner cake layer in ultrasound-treated samples (Hemmati et al., 2021).

## Effect of Ultrasound Pretreatment and Ultrasound-Assisted Ultrafiltration on Chemical Properties of Blueberry Pomace Extract

### Effect of Ultrasound Treatment on Total Phenolic Content

The TPC of the samples obtained under different ultrasound treatments was presented in Table 3. The untreated BPE exhibited a TPC of 13.69 ± 0.08 g GAE/kg LW. Similar TPC values were observed for UF and UA-UF permeates in the absence of pretreatment ($p > 0.05$).

In contrast, US-pretreatment significantly enhanced the TPC of the initial extract, increasing it to 17.15 ± 0.01 g GAE/kg LW ($p < 0.05$), corresponding to an approximately 25% increase. This enhancement can be attributed to acoustic cavitation, which generates localized high-pressure and high-shear microenvironments, leading to mechanical disruption of plant cell walls and enhanced solvent penetration. The collapse of cavitation bubbles produces microjets and shock waves that weaken structural barriers within the plant matrix, facilitating the release of bound phenolic compounds and improving mass transfer efficiency (Chemat & Khan, 2011). Consistent with this finding, Damar (2024) reported that US-pretreatment significantly increased the

**Table 3** Effect of ultrasound pretreatment and ultrasound-assisted ultrafiltration on total phenolic, flavonoid, and anthocyanin contents of blueberry pomace extract

| Sample | TPC (g GAE/kg LW) | | TFC (g CE/kg LW) | | TMAC (g Mv-3-glu/kg LW) | |
|---|---|---|---|---|---|---|
| | Untreated | US-P | Untreated | US-P | Untreated | US-P |
| BPE | $13.69 \pm 0.08^{cA}$ | $17.15 \pm 0.01^{eB}$ | $7.47 \pm 0.12^{cA}$ | $10.39 \pm 0.06^{eB}$ | $3.46 \pm 0.02^{dA}$ | $3.86 \pm 0.06^{cB}$ |
| UF feed | $11.77 \pm 0.13^{bA}$ | $12.22 \pm 0.04^{cB}$ | $6.00 \pm 0.01^{bA}$ | $6.24 \pm 0.01^{bB}$ | $3.06 \pm 0.01^{cA}$ | $3.05 \pm 0.01^{bA}$ |
| UF permeate | $7.89 \pm 0.28^{aA}$ | $9.68 \pm 0.04^{aB}$ | $4.21 \pm 0.03^{aA}$ | $4.96 \pm 0.01^{aB}$ | $2.37 \pm 0.04^{aA}$ | $2.50 \pm 0.01^{aB}$ |
| UF retentate | $14.21 \pm 0.11^{dA}$ | $13.27 \pm 0.14^{dB}$ | $7.91 \pm 0.01^{dA}$ | $6.81 \pm 0.11^{cB}$ | $2.65 \pm 0.03^{bA}$ | $3.09 \pm 0.01^{bB}$ |
| UA-UF permeate | $8.03 \pm 0.13^{aA}$ | $10.91 \pm 0.36^{bB}$ | $4.20 \pm 0.01^{aA}$ | $4.93 \pm 0.07^{aB}$ | $2.40 \pm 0.01^{aA}$ | $2.52 \pm 0.03^{aB}$ |
| UA-UF retentate | $14.77 \pm 0.05^{eA}$ | $13.67 \pm 0.04^{dB}$ | $7.90 \pm 0.02^{dA}$ | $7.01 \pm 0.02^{dB}$ | $2.67 \pm 0.01^{bA}$ | $3.12 \pm 0.03^{bB}$ |

*BPE* blueberry pomace extract, *UF* ultrafiltration, *UA-UF* ultrasound-assisted ultrafiltration, *US-P* US-pretreatment, *LW* lyophilized weight, *TPC* total phenolic content, *GAE* gallic acid equivalent, *TFC* total flavonoid content, *CE* catechin equivalents, *TMAC* total monomeric anthocyanin content, *Mv-3-glu* malvidin-3-glucoside. Different lowercase letters (a–e) within the same column indicate statistically significant differences ($p < 0.05$). Different uppercase letters (A–B) within the same row indicate statistically significant differences ($p < 0.05$)

TPC of wine production wastes, with phenolic content rising 16.4–37.6% depending on treatment duration ($p < 0.05$), demonstrating the effectiveness of ultrasound in enhancing phenolic extraction from complex plant matrices.

After pretreatment, both UF and UA-UF permeates exhibited significantly higher TPC values compared to their untreated counterparts ($p < 0.05$). Notably, the UA-UF permeate achieved $10.91 \pm 0.36$ g GAE/kg LW, representing the highest phenolic transmission among permeate fractions and suggesting a synergistic interaction between pretreatment and UA-UF. Two primary mechanisms may explain this observation. First, cavitation-induced mechanical effects can lead to partial depolymerization or structural modification of phenolic-associated macromolecular assemblies, potentially reducing their effective molecular size and facilitating passage through the 30-kDa PES membrane. Such ultrasound-induced molecular fragmentation and enhanced polyphenol permeation have been observed in related systems (Shen et al., 2023). Second, ultrasound integration during UF mitigates cake layer compaction and reduces secondary retention phenomena. In UF, the accumulated cake layer may act as a secondary selective barrier, enhancing phenolic retention beyond the intrinsic membrane cut-off. By decreasing cake layer density and compressibility, UA-UF reduces this secondary sieving effect, thus allowing a higher fraction of phenolics to permeate. For example, Aghdam et al. (2015) reported substantial reduction in cake layer thickness during ultrasound-assisted clarification, which corresponded with improved flux and reduced fouling.

Additionally, cavitation-induced shear forces may modify interactions between phenolic compounds and macromolecular components such as proteins and polysaccharides present in the extract. Disruption of these associations may inhibit the formation of larger complexes that would otherwise be retained by the membrane. Similar ultrasound-enhanced modifications in macromolecule interactions have been reported in fruit-derived extracts (dos Santos Sousa et al., 2016; Shen et al., 2023). Overall, the results indicate that US-pretreatment primarily enhances phenolic extraction efficiency, while UA-UF contributes to improved phenolic transmission by modifying fouling structure and limiting secondary retention effects at the membrane surface.

### Effect of Ultrasound Treatment on Total Flavonoid Content

The TFC of samples obtained under US-pretreatment and filtration (UF vs UA-UF) setups was presented in Table 3. The untreated BPE exhibited a TFC of $7.47 \pm 0.12$ g CE/kg LW. Similar TFC values were observed for UF and UA-UF permeates in the absence of pretreatment ($p > 0.05$).

US-pretreatment significantly increased the TFC of the initial extract from $7.47 \pm 0.12$ to $10.39 \pm 0.06$ g CE/kg LW ($p < 0.05$), corresponding to an approximately 39% enhancement. Comparable increases in flavonoid content following ultrasound-assisted extraction have been reported for blackcurrant (Gozel Yavuz & Yilmaz, 2025) and blueberry pomace (Bamba et al., 2018), confirming the effectiveness of cavitation-driven extraction in berry matrices. This enhancement is primarily attributed to cavitation-induced disruption of plant tissue structure, which promotes the release of bound flavonoid compounds and enhances mass transfer. Scanning electron microscopy (SEM) observations have further demonstrated that ultrasound treatment induces surface erosion, fragmentation, and sonoporation effects in plant tissues, facilitating compound liberation (Teixeira et al., 2023). As flavonoids constitute a major subgroup of phenolic compounds, their response to ultrasound follows similar extraction mechanisms described for TPC. Milić et al. (2022) reported that extraction techniques generally affect total phenolic and total flavonoid contents in a comparable manner due to their structural and compositional relationship.

Following pretreatment, both UF and UA-UF permeates showed approximately 18% higher flavonoid contents compared to untreated conditions ($p < 0.05$). However, no significant difference was detected between UF and UA-UF permeates under the same pretreatment condition ($p > 0.05$), suggesting that US-pretreatment primarily governs flavonoid release, whereas UA-UF mainly contributes to process stabilization rather than selective flavonoid enrichment. From a process perspective, these findings indicate that US-pretreatment enhances flavonoid availability in the feed solution, thereby improving their recovery in the permeate fraction, while the membrane step functions predominantly as a clarification and fractionation stage for these relatively low-molecular-weight compounds.

### Effect of Ultrasound Treatment on Total Monomeric Anthocyanin Content

The TMAC of samples obtained under US-pretreatment and filtration (UF vs UA-UF) setups was presented in Table 3. The untreated BPE exhibited a TMAC of $3.46 \pm 0.02$ g Mv-3-glu/kg LW. No significant difference was observed between UF and UA-UF permeates in the absence of pretreatment ($p > 0.05$). US-pretreatment significantly increased the TMAC of the initial extract to $3.86 \pm 0.06$ g Mv-3-glu/kg LW ($p < 0.05$), corresponding to an enhancement of approximately 11.6%. Similar improvements in anthocyanin content following ultrasound application have been widely reported in berry-based systems. Pradhan et al. (2022) demonstrated that ultrasound treatment increased anthocyanin concentration in Sohiong juice from 12 to 22 mg/L, while Gozel Yavuz and Yilmaz (2025) reported a 52% increase in total monomeric anthocyanin content in blackcurrant extracts using probe-type ultrasound. Likewise, He et al. (2016)

observed enhanced anthocyanin recovery from blueberry wine pomace under ultrasound-assisted extraction, attributing this effect to cavitation-induced particle collisions and cell wall disruption. Golmohamadi et al. (2013) further highlighted the frequency-dependent efficiency of cavitation, reporting increases of up to 12.6% in red raspberry extracts under low-frequency ultrasound. Collectively, these findings support the interpretation that cavitation-driven structural disintegration enhances solvent penetration and accelerates anthocyanin mass transfer from plant tissues.

Following US-pretreatment, both UF and UA-UF permeates exhibited modest but statistically significant increases (approximately 5–6%) in TMAC compared to untreated treatment ($p < 0.05$). However, no significant difference was detected between UF and UA-UF permeates under the same pretreatment condition ($p > 0.05$). To better interpret this behavior, it is important to consider molecular size and membrane selectivity. Monomeric anthocyanins (typically 400–700 Da) are substantially smaller than the 30-kDa membrane cut-off and therefore are not predominantly controlled by steric exclusion mechanisms. In UF systems, solute rejection is influenced not only by MWCO but also by physicochemical interactions between solutes and membrane materials, including π–π interactions, electrostatic forces, and van der Waals interactions (Avram et al., 2017). Cissé et al. (2011) reported that anthocyanin rejection is governed primarily by solute–membrane interactions rather than size exclusion, while Xie et al. (2022) indicated that reductions in phenolic content during UF are often associated with the retention of high-molecular-weight conjugated complexes rather than monomeric anthocyanins themselves. Although cake layer formation may contribute to overall fouling resistance, its influence on the transmission of low-molecular-weight anthocyanins appears limited compared to membrane–solute interaction effects.

Overall, the results indicate that US-pretreatment enhances anthocyanin extraction efficiency through cavitation-driven matrix disruption, while the subsequent membrane step functions primarily as a clarification and fractionation stage supporting permeate recovery without substantial degradation of monomeric anthocyanins. This observation was further supported by Linares and Rojas (2022), who reported that ultrasound-assisted extraction preserves anthocyanin integrity due to its short processing time and focused energy delivery, thereby reducing degradation associated with polymeric pigment formation.

Taken together, the results in Table 3 indicate that ultrasound pretreatment and ultrasound-assisted ultrafiltration exert different effects on total phenolic, flavonoid, and anthocyanin contents. Ultrasound pretreatment consistently increased all compound groups, which can be attributed to cavitation-induced cell disruption and enhanced mass transfer (Chemat & Khan, 2011). However, the magnitude of the increase depended on compound characteristics. Total phenolics and flavonoids showed more pronounced enhancements than anthocyanins, likely due to their broader molecular diversity and stronger association with cell wall structures. In contrast, anthocyanins, being smaller and more structurally sensitive, exhibited more moderate changes (Gozel Yavuz & Yilmaz, 2026; Shen et al., 2023).

During filtration, the role of ultrasound differed from that of pretreatment. Ultrasound-assisted ultrafiltration mainly influenced the distribution of compounds by mitigating fouling and improving mass transfer, with a more noticeable effect on phenolic transmission. Its impact on flavonoids and anthocyanins was comparatively limited, suggesting that molecular size and membrane–solute interactions are dominant factors. These findings are consistent with previous studies reporting compound-dependent responses to ultrasound and membrane processes (Avram et al., 2017; Córdova et al., 2020; Damar, 2024).

### Individual Anthocyanin Profile of Blueberry Pomace Extract

The individual anthocyanin composition of BPE under US-pretreatment and filtration (UF vs UA-UF) processing is presented in Table 4. A total of seven anthocyanin derivatives were identified and quantified, including malvidin-, delphinidin-, cyanidin-, and peonidin-based anthocyanin. In untreated BPE, the sum of identified anthocyanins was 3294.43 mg/kg LW. Malvidin derivatives dominated the profile, with Mv-3-gal accounting for ~ 31.7% and Mv-3-glu for 20.6% of total identified anthocyanins. Collectively, malvidin glycosides represented more than half of the anthocyanin fraction (~ 52%), confirming their predominance in blueberry matrices. This observation was in agreement with previous reports indicating that malvidin glycosides constitute the major anthocyanin subgroup in blueberries, accounting for more than 38% (Liu et al., 2012) and up to approximately 48% of total anthocyanins (Zhang et al., 2022). Furthermore, several studies have identified malvidin-3-galactoside as the most abundant individual anthocyanin in blueberry samples, typically ranging between 18.56 and 24.34% of total anthocyanins (Hu et al., 2019; Zhang et al., 2022). Delphinidin derivatives contributed approximately 21–22% in total, while cyanidin and peonidin derivatives constituted the remaining fraction. This distribution is consistent with the characteristic anthocyanin fingerprint reported for *Vaccinium* species, where higher methoxylation of the B-ring enhances molecular stability and contributes to the dominance of malvidin-based compounds.

Following US-pretreatment, the total quantified anthocyanins increased to 3814.48 mg/kg LW. Absolute concentrations of nearly all individual anthocyanins increased, indicating enhanced release from the plant matrix. Notably, Mv-3-gal increased from 1043.42 to 1326.39 mg/kg LW,

**Table 4** Individual anthocyanin composition of blueberry pomace extract before and after ultrasound-assisted ultrafiltration (mg/kg LW)

| Sample | Mv-3-gal | | Mv-3-glu | | Del-3-gal | | Del-3-glu |
|---|---|---|---|---|---|---|---|
| | Untreated | US-P | Untreated | US-P | Untreated | US-P | Untreated |
| BPE | $1043.42 \pm 0.29^{dA}$ | $1326.39 \pm 18.61^{dB}$ | $678.32 \pm 1.34^{fA}$ | $783.72 \pm 12.13^{dB}$ | $587.42 \pm 19.37^{dA}$ | $611.69 \pm 26.12^{dA}$ | $131.64 \pm 5.20^{cA}$ |
| UF feed | $1022.91 \pm 1.11^{cA}$ | $1282.93 \pm 1.66^{cB}$ | $610.06 \pm 0.08^{cA}$ | $759.91 \pm 2.71^{cB}$ | $559.50 \pm 0.44^{cA}$ | $600.99 \pm 2.77^{cdB}$ | $110.34 \pm 0.68^{bA}$ |
| UF permeate | $989.95 \pm 0.37^{bA}$ | $1007.59 \pm 2.11^{aB}$ | $582.20 \pm 2.06^{bA}$ | $585.16 \pm 2.41^{aA}$ | $390.82 \pm 16.34^{aA}$ | $476.99 \pm 2.57^{aB}$ | $92.73 \pm 12.14^{aA}$ |
| UF retentate | $1092.79 \pm 0.82^{eA}$ | $1270.80 \pm 1.41^{bcB}$ | $640.08 \pm 0.67^{dA}$ | $756.12 \pm 1.03^{cA}$ | $433.12 \pm 10.02^{bA}$ | $578.22 \pm 4.29^{bcB}$ | $110.01 \pm 7.38^{bA}$ |
| UA-UF permeate | $981.94 \pm 1.22^{aA}$ | $1016.61 \pm 2.31^{aB}$ | $575.87 \pm 1.12^{aA}$ | $595.12 \pm 2.71^{bB}$ | $366.80 \pm 21.31^{aA}$ | $459.25 \pm 1.89^{aB}$ | $87.71 \pm 13.67^{aA}$ |
| UA-UF retentate | $1111.81 \pm 0.88^{fA}$ | $1267.08 \pm 0.93^{bB}$ | $655.77 \pm 0.42^{eA}$ | $753.09 \pm 0.96^{cB}$ | $422.98 \pm 2.55^{bA}$ | $558.81 \pm 0.80^{bB}$ | $92.11 \pm 8.43^{aA}$ |

| Sample | Del-3-glu | Cy-3-glu | | Cy-3-rut | | Peo-3-glu | |
|---|---|---|---|---|---|---|---|
| | US-P | Untreated | US-P | Untreated | US-P | Untreated | US-P |
| BPE | $150.72 \pm 7.90^{cB}$ | $226.62 \pm 1.13^{eA}$ | $255.17 \pm 9.77^{cB}$ | $384.45 \pm 1.65^{dA}$ | $409.76 \pm 0.34^{bB}$ | $242.56 \pm 10.01^{bcA}$ | $277.02 \pm 4.36^{eB}$ |
| UF feed | $124.09 \pm 1.22^{bB}$ | $215.81 \pm 0.82^{dA}$ | $239.10 \pm 1.73^{bB}$ | $375.79 \pm 2.08^{cA}$ | $390.81 \pm 2.88^{aB}$ | $235.36 \pm 1.44^{bA}$ | $265.93 \pm 4.34^{dB}$ |
| UF permeate | $106.18 \pm 0.69^{aA}$ | $164.42 \pm 1.29^{bA}$ | $181.88 \pm 1.04^{aB}$ | $344.38 \pm 1.05^{bA}$ | $375.22 \pm 1.95^{aB}$ | $196.85 \pm 5.64^{aA}$ | $225.98 \pm 4.73^{bB}$ |
| UF retentate | $129.25 \pm 0.79^{bB}$ | $172.77 \pm 1.48^{cA}$ | $259.78 \pm 1.40^{cB}$ | $473.42 \pm 1.99^{eA}$ | $441.75 \pm 0.97^{cB}$ | $247.60 \pm 0.02^{cA}$ | $245.29 \pm 1.33^{cA}$ |
| UA-UF permeate | $104.88 \pm 0.99^{aA}$ | $157.45 \pm 0.93^{aA}$ | $181.86 \pm 1.23^{aB}$ | $339.50 \pm 1.29^{aA}$ | $375.59 \pm 11.62^{aB}$ | $201.70 \pm 5.42^{aA}$ | $217.20 \pm 2.32^{aB}$ |
| UA-UF retentate | $129.40 \pm 4.02^{bB}$ | $173.74 \pm 1.81^{cA}$ | $255.13 \pm 0.60^{cB}$ | $470.72 \pm 0.40^{eA}$ | $423.28 \pm 18.72^{bB}$ | $249.14 \pm 0.35^{cA}$ | $247.61 \pm 0.07^{cB}$ |

*US-P* US-pretreatment, *UF* ultrafiltration, *UA-UF* ultrasound-assisted ultrafiltration, *LW* lyophilized weight, *Mv-3-gal* malvidin-3-O-galactoside chloride, *Mv-3-glu* malvidin-3-O-glucoside chloride, *Del-3-gal* delphinidin-3-O-galactoside chloride, *Del-3-glu* delphinidin-3-glucoside, *Cy-3-glu* cyanidin-3-glucoside, *Cy-3-rut* cyanidin-3-rutioside, *Peo-3-glu* peonidin-3-glucoside. Different lowercase letters (a–f) within the same column indicate statistically significant differences ($p < 0.05$). Different uppercase letters (A–B) within the same row indicate statistically significant differences ($p < 0.05$)

while Mv-3-glu rose from 678.32 to 783.72 mg/kg LW. Similar increasing trends were observed for delphinidin, cyanidin, and peonidin derivatives. Despite these increases in concentration, the relative percentage distribution of anthocyanin subclasses remained largely conserved, suggesting that US-pretreatment enhanced overall extraction efficiency without inducing selective degradation or structural transformation of specific anthocyanin species. This preservation of compositional ratios is consistent with previous reports indicating that different extraction techniques, including ultrasound-assisted extraction, generally increase absolute anthocyanin yields without altering the intrinsic anthocyanin profile of berry matrices. Several studies have confirmed that, when appropriate acoustic parameters (temperature, amplitude, and treatment duration) are applied, ultrasound promotes matrix disruption while maintaining molecular integrity, and does not modify the anthocyanin fingerprint (Grace et al., 2009; He et al., 2016). These findings support the interpretation that cavitation-driven cell wall disruption primarily enhances mass transfer rather than triggering structural degradation pathways.

During UF, individual anthocyanins were detected in both UF and UA-UF permeates, confirming their transmission through the 30-kDa PES membrane. No statistically significant differences were observed between UF and UA-UF permeates for most anthocyanins ($p > 0.05$). HPLC analysis showed that US-pretreatment increased total anthocyanin recovery without altering compositional integrity, while membrane separation largely preserved the characteristic anthocyanin fingerprint, indicating that ultrasound integration did not cause selective subclass rejection or degradation.

## Antioxidant Capacity of Blueberry Pomace Extracts Under Different Ultrasound Conditions

### $ABTS^{\bullet+}$ Radical Cation Decolorization Assay

Table 5 presents the ABTS-based total antioxidant capacity (TAC-ABTS) of samples obtained under US-pretreatment and filtration (UF vs UA-UF) setups. In untreated BPE, the antioxidant capacity was $68.22 \pm 2.62$ mmol TE/kg LW. No statistically significant difference was observed between UF and UA-UF permeates in the absence of pretreatment ($p > 0.05$), indicating that ultrasound integration during filtration alone did not substantially alter antioxidant transmission.

Under US-pretreatment conditions, the antioxidant capacity of the initial extract significantly increased to $71.03 \pm 0.90$ mmol TE/kg LW ($p < 0.05$). Similar increases were observed in UF feed samples ($62.42 \pm 0.16$ mmol TE/kg LW), indicating enhanced extraction of antioxidant compounds. In permeate fractions, antioxidant capacity increased to $51.41 \pm 0.48$ mmol TE/kg LW for UF and $51.78 \pm 0.90$ mmol TE/kg LW for UA-UF. These values

**Table 5** Effect of ultrasound pretreatment and ultrasound-assisted ultrafiltration on antioxidant capacity of blueberry pomace extract determined by DPPH and ABTS assays

| Sample | TAC-ABTS (mmol TE/kg LW) | | TAC-DPPH (mmol TE/kg LW) | |
|---|---|---|---|---|
| | Untreated | US-P | Untreated | US-P |
| BPE | $68.22 \pm 2.62^{cA}$ | $71.03 \pm 0.90^{cB}$ | $63.86 \pm 0.90^{bA}$ | $64.55 \pm 0.89^{cA}$ |
| UF feed | $59.52 \pm 0.16^{bA}$ | $62.42 \pm 0.16^{bB}$ | $62.69 \pm 1.13^{bA}$ | $62.84 \pm 0.54^{cA}$ |
| UF permeate | $44.62 \pm 1.17^{aA}$ | $51.41 \pm 0.48^{aB}$ | $51.12 \pm 1.32^{aA}$ | $51.66 \pm 0.76^{aA}$ |
| UF retentate | $42.95 \pm 0.21^{aA}$ | $69.29 \pm 1.06^{cB}$ | $64.64 \pm 0.26^{bA}$ | $69.12 \pm 0.29^{dB}$ |
| UA-UF permeate | $43.78 \pm 0.28^{aA}$ | $51.78 \pm 0.90^{aB}$ | $50.68 \pm 0.36^{aA}$ | $56.29 \pm 1.59^{bB}$ |
| UA-UF retentate | $71.27 \pm 2.60^{cA}$ | $71.58 \pm 0.58^{cA}$ | $68.64 \pm 0.51^{cA}$ | $68.74 \pm 0.06^{dA}$ |

*US-P* US-pretreatment, *UF* ultrafiltration, *UA-UF* ultrasound-assisted ultrafiltration, *LW* lyophilized weight, *TAC* total antioxidant capacity, *TE* Trolox equivalent. Different lowercase letters (a–d) within the same column indicate statistically significant differences ($p < 0.05$). Different uppercase letters (A–B) within the same row indicate statistically significant differences ($p < 0.05$)

correspond to approximately 15.2% and 18.3% increases, respectively, compared to untreated permeates ($p < 0.05$). However, no statistically significant difference was observed between UF and UA-UF permeates under the same pretreatment condition ($p > 0.05$).

The observed enhancement in antioxidant capacity following US-pretreatment is consistent with the previously reported increases in total phenolic, flavonoid, and anthocyanin contents. Since antioxidant capacity represents the cumulative effect of multiple bioactive compounds, particularly phenolic constituents, the increase in TAC-ABTS values can be directly associated with the enhanced phenolic extraction efficiency. A positive correlation between total phenolic content and antioxidant capacity has been widely reported in fruit-based systems (Damar, 2024).

Similarly, ultrasound-assisted extraction has been shown to significantly enhance antioxidant capacity in berry matrices. Gozel Yavuz and Yilmaz (2025) reported approximately a 15% increase in total antioxidant capacity in blackcurrant extracts using probe-type ultrasound compared to conventional solvent extraction. In Sohiong fruit juice, Pradhan et al. (2022) observed a marked increase in radical scavenging capacity following US-pretreatment, attributing this improvement to cavitation-enhanced phenolic and anthocyanin release.

Mechanistically, cavitation-driven cell disruption is recognized as the primary factor responsible for enhanced bioactive compound recovery. The collapse of cavitation bubbles generates localized high pressure and microjets that physically disrupt plant cell walls, accelerate solvent penetration, and improve mass transfer efficiency (Chemat & Khan, 2011; Vinatoru et al., 2017). This mechanism likely contributed to the elevated antioxidant potential observed in both feed and permeate fractions.

Furthermore, the ABTS assay is known to reflect the combined and potentially synergistic activity of hydrophilic and lipophilic antioxidant compounds, making it particularly suitable for evaluating complex plant extracts (Floegel et al., 2011; Re et al., 1999). The preservation of antioxidant capacity after membrane separation therefore indicates that UF did not induce substantial oxidative degradation of active constituents.

Overall, the ABTS results demonstrate that US-pretreatment plays a dominant role in enhancing antioxidant recovery, whereas UA-UF mainly contributes to process stabilization rather than selective amplification of antioxidant capacity.

### DPPH• Radical Scavenging Activity

The DPPH-based antioxidant capacity (TAC-DPPH) of samples obtained under US-pretreatment and filtration (UF vs UA-UF) setups is presented in Table 5. In untreated BPE, the antioxidant capacity was $63.86 \pm 0.90$ mmol TE/kg LW. Similar values were observed for UF feed samples ($62.69 \pm 1.13$ mmol TE/kg LW), while lower antioxidant activities were detected in UF and UA-UF permeates ($51.12 \pm 1.32$ and $50.68 \pm 0.36$ mmol TE/kg LW, respectively). No statistically significant difference was found between UF and UA-UF permeates in the absence of pretreatment ($p > 0.05$), indicating that ultrasound integration during filtration alone did not significantly influence DPPH radical scavenging activity.

Following US-pretreatment, the antioxidant capacity of BPE slightly increased to $64.55 \pm 0.89$ mmol TE/kg LW; however, this increase was not statistically significant ($p > 0.05$). Similarly, no significant differences were observed in UF feed or UF permeate samples after pretreatment ($p > 0.05$). In contrast, the UA-UF permeate exhibited a statistically significant increase in antioxidant capacity after pretreatment ($56.29 \pm 1.59$ mmol TE/kg LW; $p < 0.05$), corresponding to an approximately 9% increase compared to the UF permeate under the same conditions.

The comparatively modest response observed in the DPPH assay relative to ABTS may reflect differences in the underlying reaction mechanisms of the two assays. While

the $ABTS^{\bullet+}$ radical cation primarily operates through an electron transfer mechanism and is applicable to both hydrophilic and lipophilic antioxidants (Floegel et al., 2011; Re et al., 1999), the $DPPH^{\bullet}$ radical generally considered more sensitive to hydrogen atom transfer capacity and steric accessibility of antioxidant molecules (Brand-Williams et al., 1995). Therefore, variations in compound composition and molecular environment may differentially influence the measured antioxidant capacity.

Similar findings have been reported in fruit-based systems. Pradhan et al. (2022) demonstrated that US-pretreatment significantly increased DPPH radical scavenging activity in Sohiong fruit juice, attributing the improvement to cavitation-induced enhancement of phenolic and anthocyanin release. In that study, antioxidant capacity increased by up to 46% following ultrasound treatment. The comparatively moderate increases observed in the present study may be related to differences in matrix composition, ultrasound intensity, and treatment duration.

In the present study, US-pretreatment produced a clearer enhancement in ABTS-derived antioxidant capacity than in DPPH-derived capacity: ABTS permeate values increased by ~ 15.2% (UF) and ~ 18.3% (UA-UF) relative to untreated permeates ($p < 0.05$), whereas DPPH showed a modest response, with a significant increase observed only for the UA-UF permeate ($56.29 \pm 1.59$ mmol TE/kg LW; $p < 0.05$). Taken together, these findings indicate that the magnitude of antioxidant enhancement after US-pretreatment is assay-dependent, consistent with the different reaction mechanisms and polarity/steric sensitivities of $ABTS^{\bullet+}$ and $DPPH^{\bullet}$ radicals. The $ABTS^{\bullet+}$ assay is suitable for evaluating both hydrophilic and lipophilic antioxidants, whereas the $DPPH^{\bullet}$ assay is more sensitive to hydrophobic compounds and is typically applied to organic-soluble extracts. In addition, $ABTS^{\bullet+}$ primarily follows an electron transfer mechanism, while $DPPH^{\bullet}$ is influenced by hydrogen atom transfer and steric accessibility of antioxidant molecules (Brand-Williams et al., 1995; Floegel et al., 2011; Re et al., 1999).

## Conclusions

This study systematically evaluated the performance of ultrasound-assisted membrane processes for the recovery of phenolic compounds and anthocyanins from blueberry pomace extract using a 30-kDa PES UF membrane. The results clearly demonstrate that US-pretreatment plays a dominant role in enhancing bioactive compound extraction, whereas ultrasound integration during UF primarily contributes to fouling mitigation and process stabilization.

US-pretreatment significantly increased total phenolic, flavonoid, and monomeric anthocyanin contents in the initial extract, confirming the effectiveness of cavitation-driven cell disruption in improving mass transfer and solvent penetration. Importantly, HPLC analysis revealed that while absolute anthocyanin concentrations increased, the relative distribution of individual anthocyanin subclasses remained largely preserved. This indicates that, under the applied acoustic conditions, ultrasound enhanced extraction efficiency without inducing selective degradation or modification of the intrinsic anthocyanin fingerprint.

During ultrafiltration, phenolic and anthocyanin compounds were successfully transmitted through the membrane, with permeate fractions retaining substantial antioxidant capacity. Ultrasound-assisted ultrafiltration reduced secondary retention effects associated with cake layer formation, contributing to improved transmission of selected compounds without altering overall compositional integrity. Resistance-in-series analysis confirmed that integrating ultrasound into the UF system markedly reduced cake layer formation (by up to 37%), thereby lowering total resistance and promoting a more reversible fouling profile.

Antioxidant evaluation using ABTS and DPPH assays revealed assay-dependent responses to ultrasound treatment. While ABTS results indicated a more pronounced enhancement in antioxidant capacity following pretreatment, DPPH responses were comparatively moderate, reflecting differences in reaction mechanisms and molecular sensitivity. The combined interpretation of both assays suggests that ultrasound primarily enhances the availability of electron-donating phenolic constituents without compromising structural stability.

Overall, the findings demonstrate that US-pretreatment coupled with UF represents an effective strategy for valorizing blueberry pomace by enhancing recovery of bioactive compounds while maintaining compositional integrity. This integrated approach offers potential for sustainable utilization of fruit processing by-products in functional food and nutraceutical applications. Therefore, the synergistic application of US-pretreatment and membrane processing enhances both extraction efficiency and permeate enrichment, supporting the implementation of this integrated strategy for the valorization of berry processing by-products. Future studies may explore optimization of acoustic parameters (e.g., amplitude and frequency) and long-term process performance to further improve selective recovery efficiency and scale-up feasibility.

**Acknowledgements** This research was supported by Trakya University Office of Scientific Research Projects Coordinations (TUBAP, Grant No.: 2024/46).

**Author Contributions** Emel Yilmaz: Conceptualization, Supervision, Writing – review & editing, Funding acquisition, Formal analysis, Project administration, Investigation. Irem Damar: Conceptualization, Supervision, Writing – review & editing, Funding acquisition, Formal analysis, Investigation, Visualization. Orazgul Garagulyyeva:

Investigation, Methodology, Writing – original draft. All authors reviewed the manuscript.

**Funding** Open access funding provided by the Scientific and Technological Research Council of Türkiye (TÜBİTAK). This research was supported by Trakya University Office of Scientific Research Projects Coordinations (TUBAP, Grant No.: 2024/46).

**Data Availability** The authors declare that all data supporting the findings of this study are available within the article.

## Declarations

**Ethics Approval** This article does not contain any studies with human or animal subjects.

**Competing interests** The authors declare no competing interests.

**Open Access** This article is licensed under a Creative Commons Attribution 4.0 International License, which permits use, sharing, adaptation, distribution and reproduction in any medium or format, as long as you give appropriate credit to the original author(s) and the source, provide a link to the Creative Commons licence, and indicate if changes were made. The images or other third party material in this article are included in the article's Creative Commons licence, unless indicated otherwise in a credit line to the material. If material is not included in the article's Creative Commons licence and your intended use is not permitted by statutory regulation or exceeds the permitted use, you will need to obtain permission directly from the copyright holder. To view a copy of this licence, visit http://creativecommons.org/licenses/by/4.0/.

## References

Aghdam, M. A., Mirsaeedghazi, H., Aboonajmi, M., & Kianmehr, M. (2015). Effect of ultrasound on different mechanisms of fouling during membrane clarification of pomegranate juice. *Innovative Food Science & Emerging Technologies, 30*, 127–131.

Ahmad, A. L., Che Lah, N., Ismail, S., & Ooi, B. (2012). Membrane antifouling methods and alternatives: Ultrasound approach. *Separation & Purification Reviews, 41*(4), 318–346.

Avram, A. M., Morin, P., Brownmiller, C., Howard, L. R., Sengupta, A., & Wickramasinghe, S. R. (2017). Concentrations of polyphenols from blueberry pomace extract using nanofiltration. *Food and Bioproducts Processing, 106*, 91–101.

Bacchin, P., Aimar, P., & Field, R. W. (2006). Critical and sustainable fluxes: Theory, experiments and applications. *Journal of Membrane Science, 281*(1–2), 42–69.

Bai, X., Zhou, L., Zhou, L., Cang, S., Liu, Y., Liu, R., Liu, J., Feng, X., & Fan, R. (2023). The research progress of extraction, purification and analysis methods of phenolic compounds from blueberry: A comprehensive review. *Molecules, 28*(8), Article 3610.

Bamba, B. S. B., Shi, J., Tranchant, C. C., Xue, S. J., Forney, C. F., & Lim, L.-T. (2018). Influence of extraction conditions on ultrasound-assisted recovery of bioactive phenolics from blueberry pomace and their antioxidant activity. *Molecules, 23*(7), Article 1685.

Brand-Williams, W., Cuvelier, M.-E., & Berset, C. (1995). Use of a free radical method to evaluate antioxidant activity. *LWT-Food science and Technology, 28*(1), 25–30.

Cassano, A., Donato, L., & Drioli, E. (2007). Ultrafiltration of kiwifruit juice: Operating parameters, juice quality and membrane fouling. *Journal of Food Engineering, 79*(2), 613–621.

Chemat, F., & Khan, M. K. (2011). Applications of ultrasound in food technology: Processing, preservation and extraction. *Ultrasonics Sonochemistry, 18*(4), 813–835.

Cissé, M., Vaillant, F., Pallet, D., & Dornier, M. (2011). Selecting ultrafiltration and nanofiltration membranes to concentrate anthocyanins from roselle extract (*Hibiscus sabdariffa* L.). *Food Research International, 44*(9), 2607–2614.

Córdova, A., Astudillo-Castro, C., Ruby-Figueroa, R., Valencia, P., & Soto, C. (2020). Recent advances and perspectives of ultrasound assisted membrane food processing. *Food Research International, 133*, Article 109163.

Damar, I. (2024). Effect of ultrasound pre-treatment on ultrafiltration performance in obtaining phenolic compounds from wine production wastes. *Biomass Conversion and Biorefinery, 14*(23), 30845–30856.

Dewanto, V., Wu, X., Adom, K. K., & Liu, R. H. (2002). Thermal processing enhances the nutritional value of tomatoes by increasing total antioxidant activity. *Journal of Agricultural and Food Chemistry, 50*(10), 3010–3014.

dos Santos Sousa, L., Cabral, B. V., Madrona, G. S., Cardoso, V. L., & Reis, M. H. M. (2016). Purification of polyphenols from green tea leaves by ultrasound assisted ultrafiltration process. *Separation and Purification Technology, 168*, 188–198.

Duan, Y., Tarafdar, A., Chaurasia, D., Singh, A., Bhargava, P. C., Yang, J., Li, Z., Ni, X., Tian, Y., & Li, H. (2022). Blueberry fruit valorization and valuable constituents: A review. *International Journal of Food Microbiology, 381*, Article 109890.

Ehsani, M., Doan, H., & Lohi, A. (2021). A comprehensive review of membrane fouling and cleaning methods with emphasis on ultrasound-assisted fouling control processes. *Korean Journal of Chemical Engineering, 38*(8), 1531–1555.

Floegel, A., Kim, D.-O., Chung, S.-J., Koo, S. I., & Chun, O. K. (2011). Comparison of ABTS/DPPH assays to measure antioxidant capacity in popular antioxidant-rich US foods. *Journal of Food Composition and Analysis, 24*(7), 1043–1048.

Giusti, M. M., & Wrolstad, R. E. (2001). Characterization and measurement of anthocyanins by UV-visible spectroscopy. *Current Protocols in Food Analytical Chemistry, 1*, F1. 2.1-F1. 2.13.

Golmohamadi, A., Möller, G., Powers, J., & Nindo, C. (2013). Effect of ultrasound frequency on antioxidant activity, total phenolic and anthocyanin content of red raspberry puree. *Ultrasonics Sonochemistry, 20*(5), 1316–1323.

Gozel Yavuz, G. T., & Yilmaz, E. (2025). Comparative evaluation of ultrasound-assisted and conventional extraction methods for anthocyanin recovery and antioxidant potential from blackcurrant. *Journal of Food Measurement and Characterization*. https://doi.org/10.1007/s11694-025-03793-7

Gozel Yavuz, G. T., & Yilmaz, E. (2026). Comparative evaluation of ultrasound-assisted and conventional extraction methods for anthocyanin recovery and antioxidant potential from blackcurrant. *Journal of Food Measurement and Characterization, 20*(2), 1465–1481.

Grace, M. H., Ribnicky, D. M., Kuhn, P., Poulev, A., Logendra, S., Yousef, G. G., Raskin, I., & Lila, M. A. (2009). Hypoglycemic activity of a novel anthocyanin-rich formulation from lowbush blueberry, *Vaccinium angustifolium* Aiton. *Phytomedicine, 16*(5), 406–415.

He, B., Zhang, L.-L., Yue, X.-Y., Liang, J., Jiang, J., Gao, X.-L., & Yue, P.-X. (2016). Optimization of ultrasound-assisted extraction of phenolic compounds and anthocyanins from blueberry (*Vaccinium ashei*) wine pomace. *Food Chemistry, 204*, 70–76.

Hemmati, A., Mirsaeedghazi, H., & Aboonajmi, M. (2021). The effect of ultrasound treatment on the efficiency of membrane clarification of carrot juice. *Journal of Food Processing and Preservation, 45*(1), Article e15001.

Hu, W., Gong, H., Li, L., Chen, S., & Ye, X. (2019). Ultrasound treatment on stability of total and individual anthocyanin extraction from blueberry pomace: Optimization and comparison. *Molecules, 24*(14), 2621.

Huang, T., Zhang, Y., Qiao, L., Luo, D., Ba, L., Xu, S., Meng, L., Cao, S., Wang, T., & Kou, X. (2025). Active ingredients of blueberry pomace: A comprehensive review of isolation, identification, health benefits and food applications. *Food Chemistry: X, 27*, Article 102459.

Irigoytia, M. B., Irigoytia, K., Sosa, N., de Escalada Pla, M., & Genevois, C. (2022). Blueberry by-product as a novel food ingredient: Physicochemical characterization and study of its application in a bakery product. *Journal of the Science of Food and Agriculture, 102*(11), 4551–4560.

Lamminen, M. O., Walker, H. W., & Weavers, L. K. (2004). Mechanisms and factors influencing the ultrasonic cleaning of particle-fouled ceramic membranes. *Journal of membrane science, 237*(1–2), 213–223.

Li, J., & Chase, H. A. (2010). Applications of membrane techniques for purification of natural products. *Biotechnology Letters, 32*(5), 601–608.

Linares, G., & Rojas, M. L. (2022). Ultrasound-assisted extraction of natural pigments from food processing by-products: A review. *Frontiers in Nutrition, 9*, Article 891462.

Liu, Y., Song, X., Zhang, D., Zhou, F., Wang, D., Wei, Y., Gao, F., Xie, L., Jia, G., & Wu, W. (2012). Blueberry anthocyanins: Protection against ageing and light-induced damage in retinal pigment epithelial cells. *British Journal of Nutrition, 108*(1), 16–27.

Lu, C., Bao, Y., & Huang, J.-Y. (2021). Fouling in membrane filtration for juice processing. *Current Opinion in Food Science, 42*, 76–85.

Luján-Facundo, M.-J., Mendoza-Roca, J.-A., Cuartas-Uribe, B., & Álvarez-Blanco, S. (2017). Membrane fouling in whey processing and subsequent cleaning with ultrasounds for a more sustainable process. *Journal of Cleaner Production, 143*, 804–813.

Maskooki, A., Kobayashi, T., Mortazavi, S. A., & Maskooki, A. (2008). Effect of low frequencies and mixed wave of ultrasound and EDTA on flux recovery and cleaning of microfiltration membranes. *Separation and Purification Technology, 59*(1), 67–73.

Milić, A., Daničić, T., Tepić Horecki, A., Šumić, Z., Teslić, N., Bursać Kovačević, D., Putnik, P., & Pavlić, B. (2022). Sustainable extractions for maximizing content of antioxidant phytochemicals from black and red currants. *Foods, 11*(3), Article 325.

Naji, O., Al-juboori, R. A., Khan, A., Yadav, S., Altaee, A., Alpatova, A., Soukane, S., & Ghaffour, N. (2021). Ultrasound-assisted membrane technologies for fouling control and performance improvement: A review. *Journal of Water Process Engineering, 43*, Article 102268.

Nour, V., Stampar, F., Veberic, R., & Jakopic, J. (2013). Anthocyanins profile, total phenolics and antioxidant activity of black currant ethanolic extracts as influenced by genotype and ethanol concentration. *Food Chemistry, 141*(2), 961–966.

Pradhan, D., Baishya, H., & Das, A. B. (2022). Effect of ultrasound, centrifugation, and enzymatic pretreatments on phytochemical properties and membrane fouling during microfiltration of Sohiong (*Prunus nepalensis* L.) juice. *Food Science and Biotechnology, 31*(11), 1443–1450.

Prevete, G., Carvalho, L. G., del Carmen Razola-Diaz, M., Verardo, V., Mancini, G., Fiore, A., & Mazzonna, M. (2024). Ultrasound assisted extraction and liposome encapsulation of olive leaves and orange peels: How to transform biomass waste into valuable resources with antimicrobial activity. *Ultrasonics Sonochemistry, 102*, Article 106765.

Qasim, M., Darwish, N. N., Mhiyo, S., Darwish, N. A., & Hilal, N. (2018). The use of ultrasound to mitigate membrane fouling in desalination and water treatment. *Desalination, 443*, 143–164.

Re, R., Pellegrini, N., Proteggente, A., Pannala, A., Yang, M., & Rice-Evans, C. (1999). Antioxidant activity applying an improved ABTS radical cation decolorization assay. *Free Radical Biology and Medicine, 26*(9–10), 1231–1237.

Shen, L., Pang, S., Zhong, M., Sun, Y., Qayum, A., Liu, Y., Rashid, A., Xu, B., Liang, Q., & Ma, H. (2023). A comprehensive review of ultrasonic assisted extraction (UAE) for bioactive components: Principles, advantages, equipment, and combined technologies. *Ultrasonics Sonochemistry, 101*, Article 106646.

Teixeira, B. A., Vidigal, M. C. T. R., & Stringheta, P. C. (2023). Optimization of ultrasound-assisted extraction of anthocyanins from purple tomatoes. *Ciência Rural, 54*(5), Article e20220604.

Thaipong, K., Boonprakob, U., Crosby, K., Cisneros-Zevallos, L., & Byrne, D. H. (2006). Comparison of ABTS, DPPH, FRAP, and ORAC assays for estimating antioxidant activity from guava fruit extracts. *Journal of Food Composition and Analysis, 19*(6–7), 669–675.

Tran, P. H., & Tran, T. T. (2021). Blueberry supplementation in neuronal health and protective technologies for efficient delivery of blueberry anthocyanins. *Biomolecules, 11*(1), Article 102.

Vinatoru, M., Mason, T., & Calinescu, I. (2017). Ultrasonically assisted extraction (UAE) and microwave assisted extraction (MAE) of functional compounds from plant materials. *TrAC Trends in Analytical Chemistry, 97*, 159–178.

Wang, L., Wang, Q., Li, Y., & Lin, H. (2013). Ultrasound-assisted chemical cleaning of polyvinylidene fluoride membrane fouled by lactic acid fermentation broth. *Desalination, 326*, 103–108.

Xie, X., Wang, X., Bi, X., Ning, N., Li, M., Xing, Y., & Che, Z. (2022). Effects of ultrafiltration combined with high-pressure processing, ultrasound and heat treatments on the quality of a blueberry–grape–pineapple–cantaloupe juice blend. *International Journal of Food Science and Technology, 57*(7), 4368–4379.

Zhang, L., Zhang, C., Wei, Z., Huang, W., Yan, Z., Luo, Z., Beta, T., & Xu, X. (2023). Effects of four drying methods on the quality, antioxidant activity and anthocyanin components of blueberry pomace. *Food Production, Processing and Nutrition, 5*(1), Article 35.

Zhang, X., Wang, S., Wu, Q., Battino, M., Giampieri, F., Bai, W., & Tian, L. (2022). Recovering high value-added anthocyanins from blueberry pomace with ultrasound-assisted extraction. *Food Chemistry: X, 16*, Article 100476.

**Publisher's Note** Springer Nature remains neutral with regard to jurisdictional claims in published maps and institutional affiliations.